2016

Compressed-Liquid Energy Storage with an Adsorption-based Vapor Accumulator for Solar-Driven Vapor Compression Systems in Residential Cooling

C. Mira-Hernandez
Purdue University

J. A. Weibel
Purdue University, jaweibel@purdue.edu

E. A. Groll
Purdue University

S V. Garimella
Purdue University, sureshg@purdue.edu

Mira-Hernandez, C.; Weibel, J. A.; Groll, E. A.; and Garimella, S V., "Compressed-Liquid Energy Storage with an Adsorption-based Vapor Accumulator for Solar-Driven Vapor Compression Systems in Residential Cooling" (2016). *CTRC Research Publications.* Paper 302.
http://dx.doi.org/dx.doi.org/10.1016/j.ijrefrig.2015.11.015

Compressed-Liquid Energy Storage with an Adsorption-Based Vapor Accumulator for Solar-Driven Vapor Compression Systems in Residential Cooling

Carolina Mira-Hernández, cmira@purdue.edu
Justin A. Weibel, jaweibel@purdue.edu
Eckhard A. Groll, groll@purdue.edu
Suresh V. Garimella[1], sureshg@purdue.edu

School of Mechanical Engineering, Purdue University
585 Purdue Mall, West Lafayette, IN 47907-2088 USA

ABSTRACT

A cycle-integrated energy storage strategy for vapor-compression refrigeration is proposed wherein thermo-mechanical energy is stored as compressed liquid. A compressed-liquid tank is integrated into the liquid line of the system by means of an adsorption-based vapor accumulator in the vapor line. Energy is retrieved through expansion of the compressed liquid, which allows for a tunable evaporator temperature. A thermodynamic model is developed to assess the system performance, with storage incorporated, for solar residential cooling in two locations with contrasting ambient temperature profiles. Ammonia, R134a, and propane, all paired with activated carbon as adsorbent, are evaluated. A high cold thermal energy storage density is achieved when operated with ammonia. However, the accumulator suppresses the coefficient of performance of the system because work is required to extract refrigerant from the adsorbent. Practical feasibility of the proposed storage strategy calls for the development of nontoxic refrigerant–adsorbent pairs with more favorable adsorption behavior.

[1] Author to whom correspondence should be addressed: (765) 494-5621, sureshg@purdue.edu

Keywords: cold thermal energy storage; air conditioning; vapor compression; solar cooling; adsorption

NOMENCLATURE

c refrigerant uptake, kg kg^{-1}

COP coefficient of performance

e_s''' cold thermal energy storage density, kWh m^{-3} (3600 kJ m^{-3})

h specific enthalpy, kJ kg^{-1}

$\dot{m}$ mass flow rate, kg s^{-1}

M mass, kg

p pressure, kPa

Q heat, kJ

$\dot{Q}$ heat flow rate, kW

q heat per unit mass, kJ kg^{-1}

t time, s

v specific volume, m^3 kg^{-1}

W mechanical work, kJ

$\dot{W}$ mechanical power, W

Greek

η efficiency

ρ density

Subscripts

A traditional refrigeration subsystem

ads	adsorption
adm	admissible
B	CTES refrigeration subsystem
b	adsorbent in vapor accumulator
c	condenser
e	evaporator
H	high temperature
l	liquid
L	low temperature
S	isentropic
sur	surroundings
v	vapor

1 Introduction

Global concerns about the environmental impact and finite availability of conventional energy sources have motivated efforts to develop technologies that harness clean and renewable energy sources. However, renewable sources are often challenged by their inherently intermittent nature. Energy from renewable sources is not always available in a useful form when demanded, and energy storage strategies are necessary to align supply with demand. In this context, solar cooling technologies appear promising because of the direct relationship between cooling load and solar radiation intensity (Kim and Infante-Ferreira, 2008). Solar radiation intensity strongly correlates with the ambient temperature and hence, cooling load is considerably higher during insolation hours and generally reaches a maximum value shortly after solar noon. This partial alignment of solar radiation intensity and cooling load thus reduces the required energy storage capacity.

Cold thermal energy storage (CTES), or the process of storing cooling capacity (ASHRAE, 2007), is relevant in a variety of refrigeration applications including solar cooling. Cold thermal energy storage serves to decouple cooling from power consumption. It can be used to shave and/or shift electricity peak demand in conditioned spaces, such as commercial buildings and residences (Chen et al., 2009; Reddy et al., 1991; Saito, 2002). Alternatively, CTES can supply cooling capacity when the energy source is unavailable, as may be the case for refrigeration systems powered by variable renewable energy sources or in the transportation of temperature-sensitive items.

Established CTES technologies include storage systems using chilled water, ice, and other phase change materials (PCM). Water-based storage technologies are mature and commercially available in view of the advantageous thermal properties, chemical stability,

wide availability, and low cost of water (Oró et al., 2012; Rismanchi et al., 2012). Sensible cold energy storage in water demands few modifications to conventional refrigeration systems and has a lower initial cost; however, large system volumes are required due to the low energy storage density (Rismanchi et al., 2012). To bring about stratification inside the chilled water storage tank, charging temperatures should exceed the water-density maximum of 4 °C (ASHRAE, 2007; Saito, 2002), restricting the temperature range and reducing the storage density. Ice storage systems, which have much higher storage densities, require charging temperatures below the freezing point of water, between -12 °C to -3 °C (Rismanchi et al., 2012; Wang and Kusumoto, 2001). This temperature range is significantly colder than the typical evaporator temperature in air-conditioning systems (Oró et al., 2012; Saito, 2002), and has an adverse effect on thermal performance. Moreover, ice storage systems have other technological challenges, such as the need for methods to control ice nucleation, processes that prevent adhesion of the ice to the cooling surface, approaches for maintaining the fluidity of ice-water mixtures, and methods to effectively melt the ice, among others (Saito, 2002). Other PCMs, such as eutectic salt solutions and organic compounds, can offer a range of different charging temperatures, but have other limitations. In general, eutectic salt solutions have good thermal properties and low cost, but are chemically unstable and corrosive (Oró et al., 2012). Organic PCMs are chemically stable, but are more expensive and have less favorable thermophysical properties (such as low thermal conductivity, low latent heat of fusion, and large change in density between solid and liquid phases) (Oró et al., 2012).

In air conditioning systems, CTES technologies are beneficial due to the inherently variable nature of the cooling load, which is dominated by daily and seasonal variations in environmental conditions and by user habits. In many areas in the United States, the

maximum electrical peak demand occurs during the summer time due to air-conditioning demand. This is especially so in regions where winter demand is met in part by the use of gas or oil for space heating (Reddy et al., 1991). In the absence of energy storage, electricity must always be produced on demand, and electrical power plants need to be oversized accordingly, leading to inefficient operation of expensive facilities (Chen et al., 2009).

The residential sector, which has a 24% share of the final energy consumption worldwide (Ürge-Vorsatz et al., 2015), is a viable niche for solar cooling with energy storage. Residences are usually spread out over large areas and have considerable roof area, traits that are compatible with distributed solar energy collection. Furthermore, energy consumption for worldwide residential heating and cooling is projected to increase by around 80% between 2010 and 2050 due to an increase in the number of households, and rising income levels leading to increased ownership of cooling equipment (Isaac and van Vuuren, 2009; Ürge-Vorsatz et al., 2015). Due to its high initial cost, the use of solar cooling is currently rare (Kim and Infante-Ferreira, 2008), and is typically restricted to commercial buildings, where total cooling demand is large and net savings offer a favorable economic return.

Although solar availability partially overlaps with air conditioning cooling load, the two are not perfectly coincident, and a compatible energy storage strategy is required to fully meet cooling demand with a solar collector of reasonable area. Solar cooling technologies include solar electric, solar thermo-mechanical, and solar thermal. In solar-electric cooling, such as electrically driven vapor compression and thermoelectric refrigeration (Kim and Infante-Ferreira, 2008; Sarbu and Sebarchievici, 2013), photovoltaic panels are used for electricity generation with batteries incorporated for energy storage

(Sarbu and Sebarchievici, 2013). The cost competitiveness of this system is favored as prices of photovoltaic modules continually decrease (Bazilian et al., 2013; Lang et al., 2013); additional benefits are realized for systems with commercial vapor-compression refrigeration units, because of the standard prices and the high coefficient of performance (COP) that facilitates the use of smaller collection areas (Otanicar et al., 2012). However, electrical energy storage in batteries is still expensive compared with thermal strategies for energy storage. Solar thermal refrigeration technologies predominantly include closed and open sorption systems, but thermo-mechanical refrigeration systems that use a steam ejector have also been considered (Kim and Infante-Ferreira, 2008; Sarbu and Sebarchievici, 2013). Although this group of technologies is compatible with commercial solar collectors used for solar heating, commercial thermal refrigeration units are scarce, and those that exist are expensive and exhibit low COP (Otanicar et al., 2012). However, thermal refrigeration systems can incorporate cold thermal energy storage strategies that are less expensive compared to electrical energy storage in batteries; alternatively, cycle-integrated storage strategies can be proposed. For example, for open sorption refrigeration with desiccants, cooling capacity may be stored through storage of hygroscopic solutions with low water content (Sarbu and Sebarchievici, 2013).

In the present study, a new strategy for cycle-integrated energy storage in vapor compression systems is proposed. The basic principle of this technology is to store compressed-liquid refrigerant, which can be expanded when cooling is required. Cooling is achieved through change of phase of the expanded liquid in a conventional evaporator. The proposed strategy addresses key limitations in the available energy storage technologies for solar electric residential refrigeration through vapor compression by providing high energy storage density, tunable temperature range of energy recovery, and a potentially lower-cost

solution. The performance and size of a solar electric refrigeration system with the proposed energy storage strategy are investigated for an average American house in the summer at two locations with contrasting ambient daily temperature profiles. The assessment is performed using a thermodynamic model and considering different refrigerant-adsorbent pairs.

2 System description

The cycle-integrated energy storage concept for vapor compression refrigeration uses excess available electricity, generated during low cooling load periods, to compress additional refrigerant vapor, which is condensed and stored at a constant pressure so that it can be expanded and evaporated at a later time when cooling is required in the absence of adequate electricity generation. An adsorption process allows densification and storage of the resulting discharged vapor. Figure 1 presents a schematic illustration of a vapor-compression system along with the additional components required for the proposed CTES storage subsystem. The primary modifications to the conventional vapor-compression refrigeration system are the inclusion of a compressed-liquid storage tank downstream of the condenser and an adsorption-based vapor accumulator downstream of the evaporator. When excess electricity is available, an additional compressor extracts vapor refrigerant from the vapor accumulator, and increases the pressure up to the condenser pressure. The vapor refrigerant is liquefied in the condenser and stored at close to ambient temperature and at constant pressure in the expandable liquid storage tank. When cooling is required, the stored compressed liquid refrigerant is expanded into the evaporator to produce the cooling effect. The refrigerant vapor exiting the evaporator is accumulated in the vapor accumulator containing a material of high adsorption affinity.

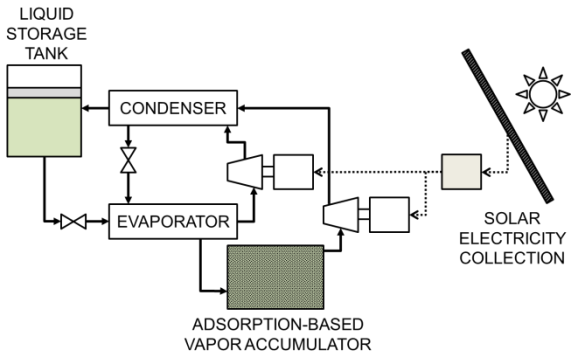

Figure 1 Schematic illustration of a vapor-compression system with compressed-liquid energy storage.

The actual vapor storage bed must be engineered to promote thermal equilibrium by dissipating/absorbing heat to/from the surroundings during the adsorption/desorption processes. Under these conditions, an ideal adsorption and desorption process traces an adsorption isotherm at the ambient temperature, and the pressure inside the vapor storage bed varies with vapor mass uptake. The system operation is designed such that the minimum pressure in the vapor adsorption bed is atmospheric and the maximum pressure is that of the evaporator. In this way, the accumulator never operates in a vacuum to prevent leakage of ambient air into the system, and ensures the existence of a pressure gradient to promote vapor flow into the adsorption bed.

The components of a traditional vapor-compression refrigeration system are maintained with some modifications. For example, the evaporator and condenser may need to be resized to operate with variable and larger flow rates during charge and discharge of the CTES subsystem. Also, it is necessary to include a separate compressor and a separate expansion valve for the storage equipment so that the traditional refrigeration subsystem may operate during charging of the storage subsystem. In this situation, the pressure in the vapor accumulator may differ from the pressure at the evaporator exit. Moreover, special

attention should be paid to the compressor design to handle the variable load and to prevent clogging of the adsorption bed with lubricant oil. Variable-speed compressors are an attractive option because they can adapt to variable requirements in mass flow rates, available energy and operating pressures. Additional implementation of a pressure-regulating valve to equalize the pressure at the compressor inlet may suppress the need of an additional compressor (with the attendant penalty to energy efficiency).

In the interest of maintaining good system thermal performance, cooling with the traditional refrigeration subsystem is always prioritized during operation, because deploying the storage subsystem is less efficient due to irreversibility in the adsorption/desorption cycle. Also, the system is operated under the premise that cooling demand is always satisfied. If the available electricity perfectly matches the amount required to meet the cooling load, only the compressor in the traditional refrigeration subsystem operates. If there is an excess of available electricity, the CTES subsystem compressor operates to extract the vapor from the accumulator and charge the liquid refrigerant storage tank. When cooling is not required to keep the conditioned space at a set-point temperature, charging of the storage tank can occur separately. If the available electricity is insufficient to meet the cooling load, the liquid refrigerant storage tank is discharged to assist in providing additional cooling. When there is no electricity available, the storage subsystem is operated independently to meet the cooling load. Table 1 summarizes the different configurations of the system during operation under different conditions of cooling load and available electricity. Electricity availability may vary either due to an intermittent renewable energy source or due to variable pricing schemes in conventional electric grids which are intended to shave or shift peak electricity consumption.

Table 1 Operating modes of refrigeration system with compressed-liquid energy storage.

Condition	Operating mode
$\dot{W}_{available} = \frac{\dot{Q}_L}{COP_t}$	Steady-flow operation of traditional refrigeration subsystem
$\dot{W}_{available} > \frac{\dot{Q}_L}{COP_t}$ and $\dot{Q}_L > 0$	Simultaneous charge of storage subsystem with steady-flow operation of traditional refrigeration subsystem
$\dot{W}_{available} > \frac{\dot{Q}_L}{COP_t}$ and $\dot{Q}_L \leq 0$	Charge of storage subsystem
$\dot{W}_{available} < \frac{\dot{Q}_L}{COP_t}$ and $\dot{W}_{available} > 0$	Simultaneous discharge of storage subsystem with steady-flow operation of traditional refrigeration subsystem
$\dot{W}_{available} = 0$ and $\dot{Q}_L > 0$	Discharge of storage subsystem

3 Analysis

3.1 Thermodynamic analysis

The behavior of the system is analyzed with a thermodynamic model that considers ideal quasi-equilibrium processes. In the model, it is assumed that the vapor refrigerant is saturated at the evaporator outlet, and that the liquid refrigerant is saturated at the condenser outlet. Also, the liquid storage tank and the vapor adsorption accumulator are assumed to be fixed at the ambient temperature. The heat exchangers (evaporator and condenser), compressors, and expansion valves are modeled as steady-flow devices without mass/energy accumulation. Figure 2 shows a thermodynamic diagram of the vapor-compression cycle with the proposed CTES subsystem included and Table 2 presents a list of the thermodynamic states.

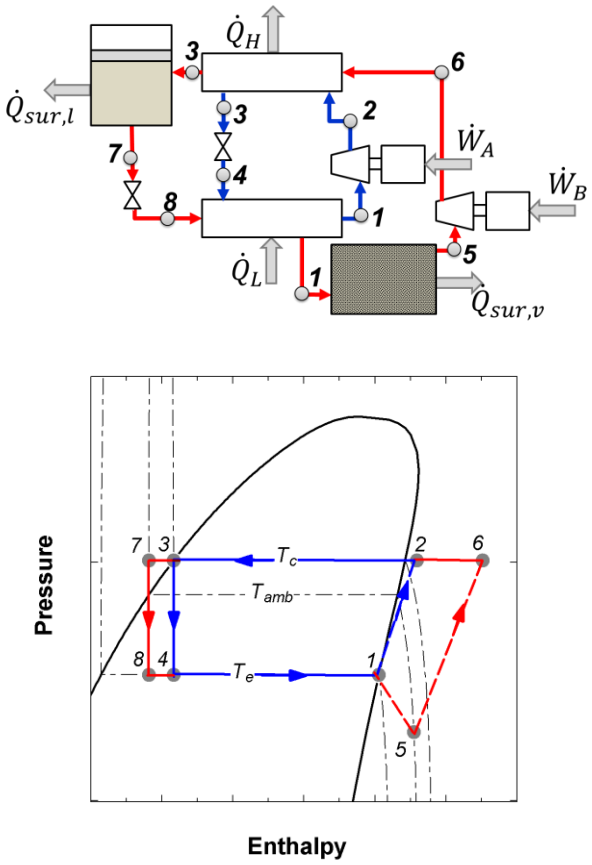

Figure 2 Thermodynamic diagram of the vapor-compression refrigeration cycle with compressed-liquid energy storage.

Table 2 Thermodynamic states for refrigeration system with compressed-liquid energy storage.

State	Location	Phase	Properties
1	Evaporator exit	Saturated vapor	$x = 1$ and $p = p_e$
2	Compressor exit in traditional subsystem	Superheated vapor	$h = h_2$ and $p = p_c$
3	Condenser exit	Saturated liquid	$x = 0$ and $p = p_c$
4	Expansion valve exit in traditional subsystem	Saturated mixture	$h = h_3$ and $p = p_e$
5	Adsorption-based vapor accumulator	Adsorbed vapor	$T = T_{amb}$ and $c = \frac{M_v}{M_b}$
6	Compressor exit in storage subsystem	Superheated vapor	$h = h_6$ and $p = p_c$
7	Liquid refrigerant storage tank	Subcooled liquid	$T = T_{amb}$ and $p = p_c$
8	Expansion valve exit in storage subsystem	Saturated mixture	$h = h_7$ and $p = p_e$

The evaporator and condenser operate at constant pressure and it is assumed that incoming flow streams mix adiabatically. The rate of cooling is

$$\dot{Q}_L = \dot{m}_A(h_1 - h_4) + \dot{m}_{B,e}(h_1 - h_8), \quad (1)$$

and the rate at which heat is rejected from the condenser is

$$\dot{Q}_H = \dot{m}_A(h_2 - h_3) + \dot{m}_{B,c}(h_6 - h_3). \quad (2)$$

Expansion of the liquid refrigerant occurs adiabatically ($h_3 = h_4; h_7 = h_8$). The mass flow rates of the incoming streams to the condenser are controlled by the power input in the compressor, and are determined as:

$$\dot{W}_A = \dot{m}_A(h_2 - h_1) \quad (3)$$

$$\dot{W}_B = \dot{m}_{B,c}(h_6 - h_5) \quad (4)$$

The total power input to the system is equal to the available power:

$$\dot{W}_{available} = \dot{W}_A + \dot{W}_B \quad (5)$$

An isentropic efficiency of 85% is assumed for the compression processes:

$$\eta_{c,A} = \frac{h_{2s} - h_1}{h_2 - h_1} \quad (6)$$

$$\eta_{c,B} = \frac{h_{6s} - h_5}{h_6 - h_5} \quad (7)$$

Mass and energy balances in the liquid storage tank are expressed as

$$\frac{dM_l}{dt} = \dot{m}_{B,c} - \dot{m}_{B,e} \quad (8)$$

$$h_7 \frac{dM_l}{dt} = h_3 \dot{m}_{B,c} - h_7 \dot{m}_{B,e} + \dot{Q}_{sur,l} \tag{9}$$

Similarly, mass and energy balances for the vapor adsorption accumulator are expressed as

$$\frac{dM_v}{dt} = \dot{m}_{B,e} - \dot{m}_{B,c} \tag{10}$$

$$q_{ads} \frac{dM_v}{dt} = h_5 \dot{m}_{B,c} - h_1 \dot{m}_{B,e} + \dot{Q}_{sur,v} \tag{11}$$

The pressure inside the vapor adsorption accumulator is determined from the adsorption isotherm for the specific refrigerant-adsorbent pair ($p_5 = f(T_{amb}, c)$). The thermodynamic model is solved using Engineering Equation Solver (EES) (Klein and Alvarado, 1992).

3.2 Storage subsystem metrics and refrigerant-adsorbent selection

The energy storage density of the storage subsystem depends on the operating conditions and materials selected for CTES. The gross volume of the subsystem comprises the volumes of the liquid storage tank and the vapor adsorption accumulator. The CTES density can therefore be estimated as:

$$e_s''' = \frac{1}{(h_1 - h_7)} \left(v_7 + \frac{1}{\rho_b \Delta c_{adm}} \right) \tag{12}$$

where Δc_{adm} represents the change in refrigerant uptake in the adsorbent across the admissible pressure range, *i.e.*, between atmospheric pressure and the evaporator pressure.

To increase CTES density, it is desirable to have a large heat of vaporization, a high bulk density of the adsorbent, a high-density compressed-liquid refrigerant, and a high adsorption isotherm slope in the admissible pressure range.

As mentioned in the model description, the pressure inside the adsorption bed is determined by the adsorption isotherm, and thus varies during the CTES subsystem charging process. Hence, the amount of mechanical work required to charge the storage depends on the refrigerant-adsorbent pair. The storage subsystem coefficient of performance serves to quantify the penalty in thermal performance due to the inclusion of the CTES:

$$COP_B = \frac{Q_{L,B}}{W_B} = \frac{(h_1 - h_7)\Delta c_{adm}}{\int_{\Delta c_{adm}} (h_6 - h_5)\, dc} \tag{13}$$

Ideally, the storage medium (in this case the refrigerant) should be commonly available, low-cost, environmentally benign, non-flammable, non-explosive, non-toxic, non-corrosive, and inert (ASHRAE, 2007). None of the existing and widely used refrigerants considered for this study fulfill all of these requirements, and technological controls must be implemented to reduce the risk of leaks and emissions. Hydrofluorocarbons, such as R134a and R410A, were developed to replace chlorofluorocarbons because of their contribution to ozone depletion; however, both families of synthetic refrigerants have a high global warming potential (Calm, 2008). Climate change concerns have promoted a renewed interest in natural refrigerants, which include hydrocarbons, carbon dioxide, and ammonia (Riffat et al., 1997). Hydrocarbons, such as propane, ethane, and butane, are flammable (ASHRAE, 2009), but pure isobutane and isobutane blends are very common in domestic refrigerators in Europe (Calm, 2008). Ammonia has no ozone depletion or global warming potential, is low cost, and is an excellent refrigerant in terms of thermodynamic and transport properties (Lorentzen, 1995; Riffat et al., 1997). Nevertheless, ammonia is classified as a hazardous material, and strict

safety controls would be required for residential use (Cengel and Boles, 2011; OSHA, 2011).

To assess the viability of the proposed CTES strategy, refrigerants R134a, propane, and ammonia adsorbed onto activated carbons are considered that span across synthetic and natural refrigerants. The analysis uses measured adsorption data that are available in the literature for different types of activated carbon. For R134a, the adsorption isotherms for the commercial activated carbon Maxorb III are used (Loh et al., 2012). For propane, experimental adsorption data for extruded activated carbon are fitted onto Dubinin-Astakhov isotherms (Esteves et al., 2008). For ammonia, reported adsorption isotherms for monolithic activated carbon are used (Critoph, 1996). The objective of the current study is not to exhaustively evaluate all possible refrigerant-adsorbent pairs, but to understand the general behavior of the storage subsystem with available pairs, assess the technological potential, and establish material development guidelines for this cycle-integrated storage strategy.

3.3 Solar residential cooling application

The current study considers a specific refrigeration application to evaluate the potential size and performance of the proposed energy storage strategy. A residential air-conditioning system powered with solar energy is selected as a promising application because it requires only moderate energy storage to fully meet the energy demand with a reasonable solar collection area.

For the analysis, the cooling load during a typical summer day is defined for two different locations for a standard American house. The basic parameters of the house, presented in Table 3, are taken from a U.S. Department of Energy study of construction

codes (Mendon et al., 2013). The selected locations are Miami, Florida, and Sacramento, California. Weather data from a typical meteorological year (TMY3) (NREL, 2015) are averaged over the month of July to represent a typical summer day in these locations. These locations were selected due to their contrasting temporal ambient temperature profiles. In Miami, where the average ambient temperature (28.1 °C) and relative humidity are high, the ambient temperature has a moderate variation between daytime and nighttime (6.0 °C). In Sacramento, where the climate is dry with mixed temperatures, the ambient temperature has a more extreme variation between daytime and nighttime (18.3 °C) but is lower on average (23.8 °C). Table 4 presents climatological parameters for the two locations during a typical summer day.

Table 3 Basic parameters of standard house for cooling load estimation (Mendon et al., 2013).

Parameter	Value
Architecture	Simple rectangular building
Footprint and height	30 ft (9.1 m) × 40 ft (12.2 m), two-story 8.5 ft-(2.6 m) high ceilings
Conditioned floor area	2400 ft^2 (223 m^2)
Window area	15% of wall area, equally distributed
Roof	Gabled with 4:12 slope, medium colored asphalt shingles
Foundation type	Slab on grade
Construction type	Lightweight

Table 4 Climatological parameters in selected locations during average summer day.

Parameter	Sacramento	Miami
Latitude, ϕ [°]	38.7	25.8
Longitude, ψ [°]	-121.6	-80.3
Altitude, H $[m]$	7	11
Mean ambient temperature, $\bar{T}_{amb}$ $[°C]$	23.8	28.1
Minimum ambient temperature, $T_{amb,min}$ $[°C]$	15.6	25.5

Maximum ambient temperature, $T_{amb,max}$ $[°C]$	33.9	31.5
Daily solar radiation on tilted to latitude south facing surface, $\bar{H}_T$ $[kWh\ m^{-2}\ day^{-1}]$	7.5	5.8

The cooling load profile in the two locations is estimated using the radiant time series method. The standard house is examined as a single zone with constant temperature of 24 °C. General guidelines from ASHRAE for cooling load computation of lightweight construction are followed (ASHRAE, 2009). The model includes external energy gain, occupancy loads, and ventilation. External energy gain is composed of heat transfer through the roof, external walls, and fenestration. Occupancy loads include heat dissipation from lighting, occupants, kitchen appliances, clothes washer, clothes dryer, and miscellaneous electric equipment; the profiles of these loads during the day are taken from (Mendon et al., 2013). The ventilation heat load is predicted neglecting strategies for recovering energy from discharged air, and imposing three air changes per hour (ASHRAE, 2009).

For both locations, the evolution of ambient temperature and solar irradiation throughout the day, along with the estimated cooling load profile, are inputs to the thermodynamic analysis of the vapor-compression system with energy storage. Evaporator and condenser temperatures of 4 °C and 40 °C, respectively, are assumed. The solar collection area and size of the storage subsystem are determined under the premises that cooling load is entirely met with solar energy and the operating pressure of the adsorption-based vapor accumulator is maintained between the evaporator pressure and the ambient pressure. An efficiency of 15% is assumed for photovoltaic solar energy conversion, and it is assumed that the panels are positioned facing south and with an angle from horizontal equal to the latitude of the particular location.

4 Results and Discussion

4.1 Cold thermal energy storage density

The CTES density is estimated for the proposed strategy with each different refrigerant considered using Equation (12), as a function of evaporator temperature, as shown in Figure 3. Storage density increases almost linearly with evaporator temperature: Evaporator pressure increases with temperature, enlarging the operating range of the storage subsystem, and thus boosting the refrigerant uptake in the adsorption bed. This trend is opposite to the behavior in chilled water storage, where energy storage density decreases with evaporator temperature due to the smaller temperature difference available for sensible heat storage. The CTES density for the system with compressed-liquid energy storage is also sensitive to the ambient temperature at which the liquid storage tank and the vapor accumulator are maintained, but is insensitive to the condenser temperature. For the results in the figure, an ambient temperature of 25°C is assumed.

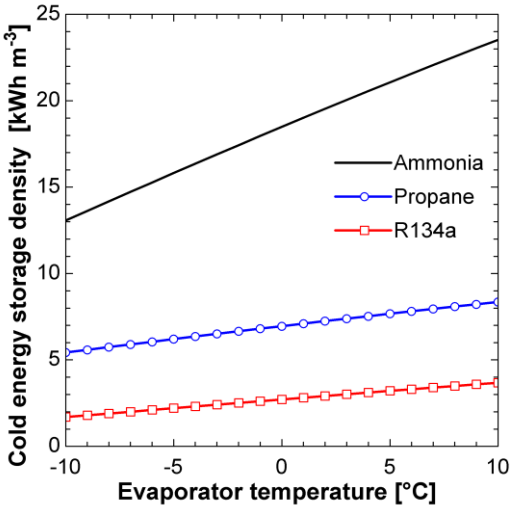

Figure 3 Cold thermal energy storage density for compressed-liquid energy storage with different refrigerants adsorbed onto activated carbon and at an ambient temperature of 25 °C.

When the storage subsystem operates with the ammonia adsorption pair, it has a dramatically higher CTES density due to the much larger vaporization enthalpy and the high bulk density of the monolithic activated carbon. For the R134a adsorption pair, the subsystem has a poor CTES density because of the low vaporization enthalpy and the use of non-agglomerated activated carbon with low bulk density.

High CTES densities can be achieved with the proposed storage strategy at typical operating conditions for air conditioning. For an evaporator temperature of 4 °C, and with ammonia as refrigerant, the CTES density is approximately 20 kWh m^{-3}, which is higher in value than chilled water storage (~7 kWh m^{-3}), similar to phase change systems using eutectic salts (~20 kWh m^{-3}), and approximately half of ice thermal storage (~47 kWh m^{-3}) (Rismanchi et al., 2012). It is important to note that these storage density estimates are idealized and would be reduced based upon the volume occupied by auxiliary components in an actual system; in the case of the proposed storage strategy, additional equipment would need to be included to dissipate the heat of adsorption.

4.2 Storage subsystem coefficient of performance

Since isothermal extraction of the refrigerant from the adsorption bed requires additional mechanical work, meeting the cooling load using the CTES subsystem is less efficient (and the COP lower) than for operating in the conventional vapor-compression refrigeration mode (*i.e.*, the traditional refrigeration subsystem). The extent of this performance reduction depends on the affinity between the refrigerant and the adsorbent, and on the thermodynamic properties of the refrigerant. An adsorption isotherm with a high slope in the operating range, and a refrigerant with a large vaporization enthalpy are preferred. The storage subsystem COP (Equation (13)) can be used as a measure of the relative overall system performance reduction when comparing between different candidate refrigerant-adsorbent pairs. Figure 4 presents the behavior of the storage subsystem COP with respect to evaporator and condenser temperatures for the different refrigerants. A higher storage subsystem COP is found for R134a because the much larger slope of the adsorption isotherm outweighs its low vaporization enthalpy. Ammonia has a larger relative vaporization enthalpy with an adsorption isotherm slope that is similar to that of propane, which explains the performance of the CTES subsystem with ammonia versus propane.

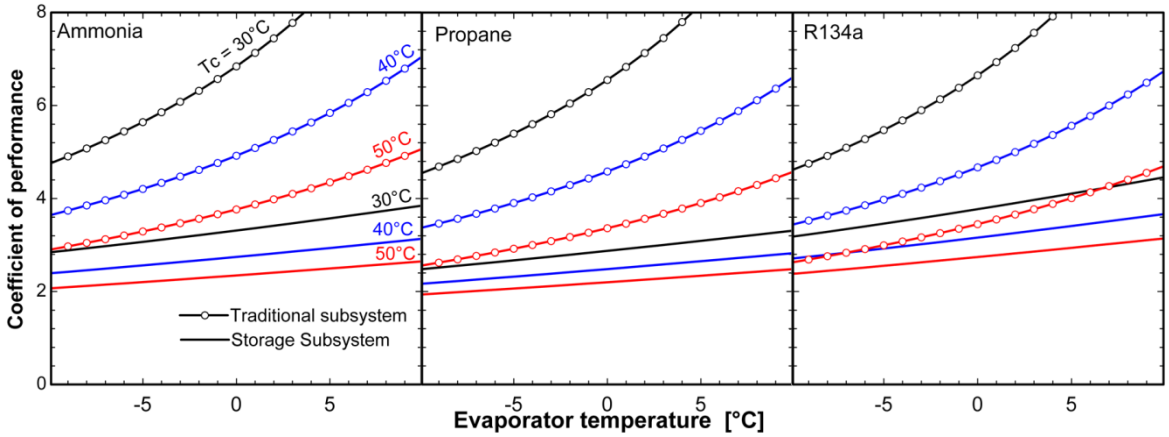

Figure 4 Coefficient of performance of the compressed-liquid storage subsystem compared with the traditional vapor compression system at an ambient temperature of 25 °C and condenser temperatures of 30 °C, 40 °C and 50 °C.

4.3 Performance of the solar residential cooling system

Figure 5 and Figure 6 present the cooling load and mechanical energy usage during the day for a solar residential air conditioning system using the proposed energy storage subsystem in Sacramento, California, and in Miami, Florida, respectively. As can be seen from the right axis, the cooling load tracks the ambient temperature; the maximum load is shifted towards the afternoon hours after the peak solar energy availability when the ambient temperature is a maximum. This highlights the need for a CTES strategy in solar air conditioning applications. In Sacramento, a location with a more dramatic temperature variation between day and night, cooling is not required during most of the night and only 2.5% of the total cooling load is required outside solar insolation hours; however, the maximum cooling load occurs in the afternoon with a lag of 4 h after the maximum solar energy availability. In this location, the primary function of the CTES subsystem is to compensate for the lag between solar availability and cooling load. The CTES subsystem is charged during the first few hours of the morning and discharged at the end of the afternoon. The traditional refrigeration subsystem plays an important role at around

midday and during the early afternoon, when more overlap exists between solar availability and cooling load.

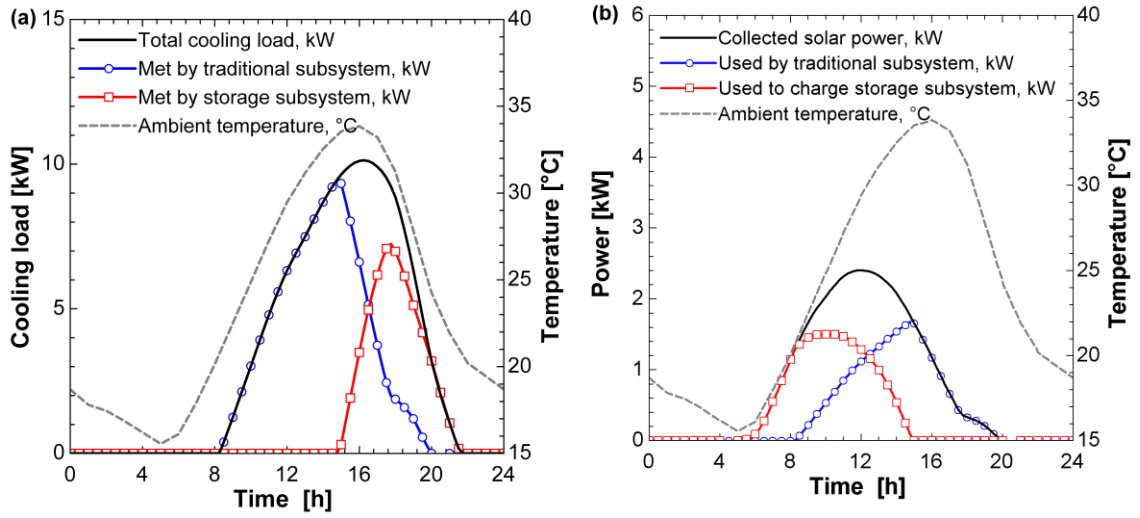

Figure 5 (a) Cooling load and (b) solar power consumption for the refrigeration system with compressed-liquid energy storage in Sacramento, California.

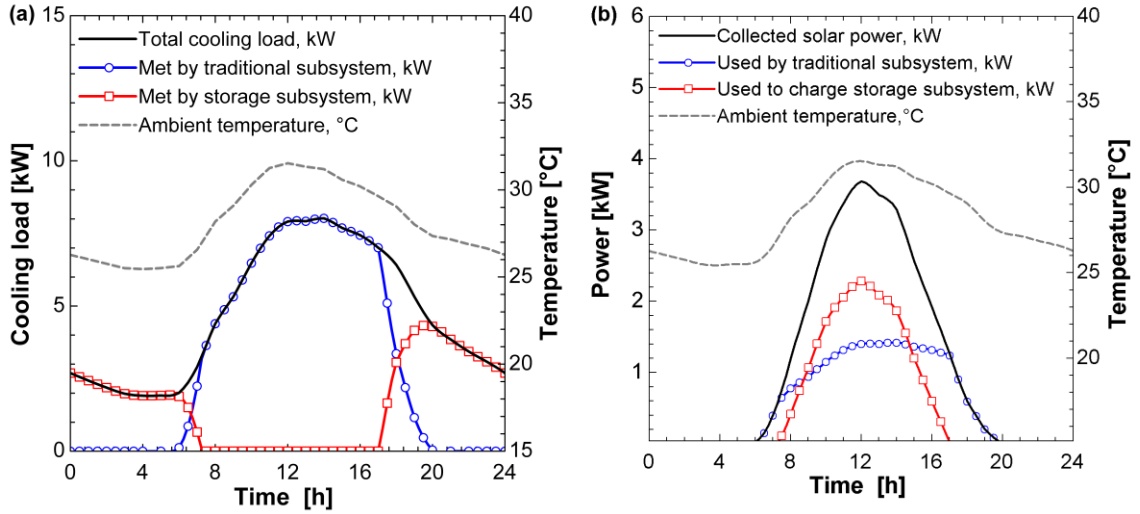

Figure 6 (a) Cooling load and (b) solar power consumption for the refrigeration system with compressed-liquid energy storage in Miami, Florida.

In Miami, a location with less variation of temperature between day and night, the CTES subsystem is primarily required to meet the cooling load outside the solar insolation

hours, when 22.1% of the cooling is required; in contrast, the conventional traditional refrigeration subsystem provides cooling when solar energy is available. Charging of the CTES subsystem and operation of the traditional refrigeration subsystems occur almost simultaneously.

Table 5 summarizes the design and performance parameters for the systems operating in Sacramento and Miami, respectively. An acceptable overall solar COP is obtained in both locations (on the order of 0.7), which is comparable with other solar cooling technologies such as absorption refrigeration, which can achieve a thermal COP between 0.5 and 0.7 for heat source temperatures between 80 and 110 °C (Srikhirin et al., 2000). However, the proposed refrigeration system with cycle-integrated storage can adapt to mismatches between solar availability and cooling load, yielding a higher fraction of solar energy utilization to meet the cooling demand with the same solar collection area. In the particular case being analyzed, the solar cooling system with storage is designed such that the entire cooling load is met using solar energy, *i.e.*, a solar fraction of unity, and the storage subsystem enables approximately 33% of the cooling. A larger system is required in Miami than Sacramento (31 m^2 versus 17 m^2 of collection area) because the daily cooling load for the typical house design is 42% larger and the available solar energy is lower (5.8 kWh m^{-2} day^{-1} versus 7.5 kWh m^{-2} day^{-1}). However, the overall solar COP of the system in both locations is very similar.

Table 5 Summary of performance parameters for the solar cooling system with compressed-liquid energy storage in selected locations operating with ammonia adsorbed on activated carbon.

Performance parameter	Sacramento	Miami
Energy		
Total consumption of mechanical energy, kWh	18.7	26.9
Fraction of mechanical energy consumed by traditional refrigeration	0.515	0.504
Fraction of mechanical energy consumed to charge storage subsystem	0.485	0.495
Total cooling load, kWh	80.6	114.1
Fraction of cooling load met by traditional subsystem	0.672	0.670
Fraction of cooling load met by storage subsystem	0.328	0.330
Mechanical COP of storage subsystem	2.93	2.83
Overall solar COP	0.65	0.64
Mass		
Total mass of refrigerant, kg	181	258
Dead mass of refrigerant, kg	99	139
Mass of activated carbon, kg	808	1217
Size		
Solar collection area, m^2	16.6	31.1
Volume of liquid refrigerant tank, m^3	0.14	0.20
Volume of adsorption based vapor accumulator, m^3	1.13	1.71
Cold thermal energy storage density, kWh m^{-3}	20.8	19.8

Although the CTES density of the proposed storage strategy is high compared with existing alternatives, the size of the storage subsystem for the proposed application is large due to the magnitude of the total cooling load. Among the refrigerant-adsorbent pairs under consideration, monolithic activated carbon with ammonia yields the most compact subsystem due to the high bulk density of monolithic activated carbon. Hence, the analysis of the solar residential cooling system is performed with this refrigerant-absorbent pair. The total volume of the storage subsystem is 1.27 m^3 and 1.91 m^3 in Sacramento and Miami, respectively. The volume of the liquid storage tank for the system operating in Miami is 0.2 m^3, which is a reasonable size for a pressurized container and comparable to

the volume of a water heater tank. The largest component of the storage subsystem is the vapor adsorption accumulator, which accounts for 90% of the subsystem volume. For the residential cooling application, the vapor accumulator may be located outdoors due to its size and because of its operation at ambient temperature.

The vapor adsorption accumulator needs to be partially saturated with refrigerant to avoid operation at vacuum pressure. The quantity of refrigerant that does not participate in the cooling process but must remain in the accumulator, denoted as the "dead mass" of refrigerant, is a disadvantage of the proposed strategy. Using ammonia also results in the lowest dead mass of refrigerant (139 kg in Miami), which is modest compared to the impractical values obtained when propane (739 kg) or R134a (1650 kg) are considered. This is explained by the lower refrigerant uptake at atmospheric pressure for the ammonia-activated carbon pair under consideration.

Figure 7 presents the evolution of absolute pressure inside the vapor adsorption accumulator along with the net mass flow rate for systems operating with ammonia in Sacramento and Miami. As a result of the dead mass of refrigerant, the pressure is bounded between the atmospheric pressure and the evaporator pressure. Also, following the adsorption isotherm, refrigerant vapor flow to the accumulator causes an increase in pressure inside the bed, whereas vapor extraction causes a reduction.

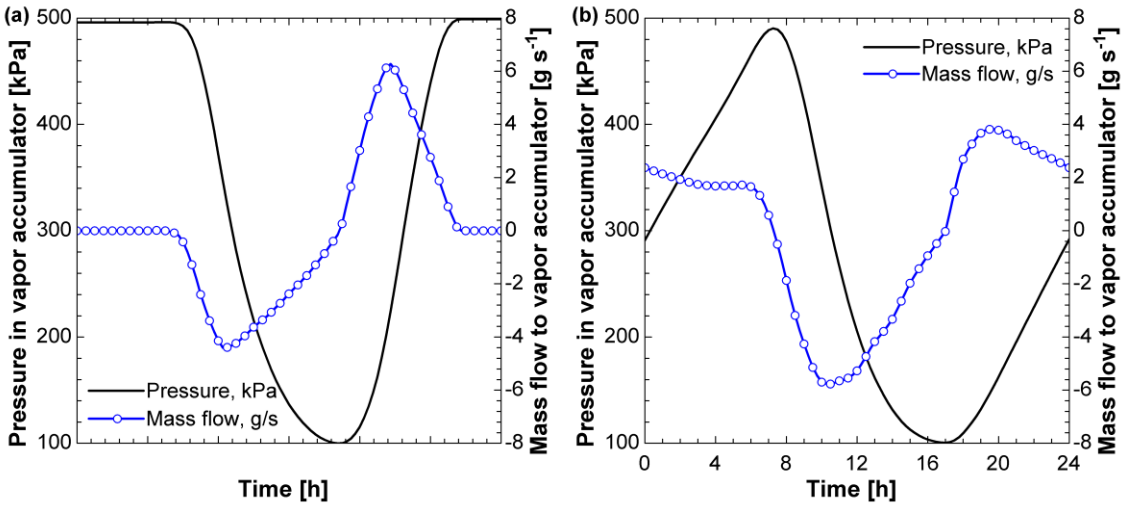

Figure 7 Pressure and net mass flow to adsorption-based vapor accumulator for compressed-liquid energy storage subsystem in (a) Sacramento, California and (b) Miami, Florida (Refrigerant: Ammonia).

5 Conclusion

A cycle-integrated CTES strategy for vapor-compression refrigeration systems is proposed. The underlying principle is to store compressed liquid refrigerant so that it can be expanded when cooling capacity is required. An adsorption-based vapor accumulator is necessary to store excess expanded vapor refrigerant when the CTES subsystem is discharged. The performance and storage capacity of the refrigeration system with compressed-liquid energy storage strongly depends on the properties of the refrigerant-adsorption pair. Therefore, materials selection and development is crucial for the viability of the proposed system. For illustration, a set of refrigerant-adsorption pairs is evaluated. The proposed CTES strategy achieves a high storage density when it operates with ammonia, and has the advantage over other technologies of a tunable temperature for energy recovery. The use of the adsorption-based accumulator imposes a penalty on thermal performance that is less severe with R134a adsorbed onto non-agglomerated activated carbon, due to the higher slope of the adsorption isotherm.

Solar residential air conditioning with photovoltaic-driven vapor compression refrigeration is considered as a specific application of the proposed strategy. The cooling load profile is computed for a typical American house on a representative summer day in two locations, and the performance and design parameters of the solar air conditioning system with storage are estimated. The cooling system with the proposed energy storage is able to fully meet the cooling load at a reasonable solar collection area for a residential application (less than 30% of the house footprint), and has an overall coefficient of performance comparable to alternative solar cooling systems. For the application, ammonia is the only working fluid with a matching adsorbent that yields a realizable size of the storage subsystem. However, ammonia raises toxicity concerns; the proposed technology calls for the development of non-toxic refrigerant-adsorbent pairs with thermophysical properties as identified by the analysis that are favorable for operation of the storage subsystem.

Acknowledgment

The first author acknowledges financial support from the Colombia-Purdue Institute (CPI) and the Colombian department for science, technology and innovation (Colciencias).

REFERENCES

ASHRAE, 2009. ASHRAE Handbook: Fundamentals. American Society of Heating, Refrigerating and Air-Conditioning Engineers.

ASHRAE, 2007. ASHRAE Handbook: Heating, ventilating, and air-conditioning applications. American Society of Heating, Refrigerating and Air-Conditioning Engineers.

Bazilian, M., Onyeji, I., Liebreich, M., MacGill, I., Chase, J., Shah, J., Gielen, D., Arent, D., Landfear, D., Zhengrong, S., 2013. Re-considering the economics of photovoltaic power. Renew. Energy 53, 329–338.

Calm, J.M., 2008. The next generation of refrigerants - Historical review, considerations, and outlook. Int. J. Refrig. 31, 1123–1133.

Cengel, Y.A., Boles, M.A., 2011. Thermodynamics: an engineering approach, 6th ed. McGraw-Hill, New York.

Chen, H., Cong, T.N., Yang, W., Tan, C., Li, Y., Ding, Y., 2009. Progress in electrical energy storage system: A critical review. Prog. Nat. Sci. 19, 291–312.

Critoph, R.E., 1996. Evaluation of alternative refrigerant—adsorbent pairs for refrigeration cycles. Appl. Therm. Eng. 16, 891–900.

Esteves, I.A.A.C., Lopes, M.S.S., Nunes, P.M.C., Mota, J.P.B., 2008. Adsorption of natural gas and biogas components on activated carbon. Sep. Purif. Technol. 62, 281–296.

Isaac, M., van Vuuren, D.P., 2009. Modeling global residential sector energy demand for heating and air conditioning in the context of climate change. Energy Policy 37, 507–521.

Kim, D.S., Infante-Ferreira, C.A., 2008. Solar refrigeration options – A state-of-the-art review. Int. J. Refrig. 31, 3–15.

Klein, S.A., Alvarado, F.L., 1992. EES: Engineering equation solver for the Microsoft Windows operating system.

Lang, T., Gloerfeld, E., Girod, B., 2013. Don’t just follow the sun - A global assessment of economic performance for residential building photovoltaic. Renew. Sustain. Energy Rev. 42, 932–951.

Loh, W.S., Ismail, A. Bin, Xi, B., Ng, K.C., Chun, W.G., 2012. Adsorption isotherms and isosteric enthalpy of adsorption for assorted refrigerants on activated carbons. J. Chem. Eng. Data 57, 2766–2773.

Lorentzen, G., 1995. The use of natural refrigerants: a complete solution to the CFC/HCFC

predicament. Int. J. Refrig. 18, 190–197.

Mendon, V., Lucas, R., Goel, S., 2013. Cost-Effectiveness Analysis of the 2009 and 2012 IECC Residential Provisions – Technical Support Document. Pacific Northwest National Laboratory, U.S. Department of Energy.

NREL, 2015. 1991- 2005 Update: typical meteorological year 3 [WWW Document]. Natl. Sol. Radiat. Data Base. URL http://rredc.nrel.gov/solar/old_data/nsrdb/1991-2005/tmy3/ (accessed 5.29.15).

Oró, E., de Gracia, A., Castell, A., Farid, M.M., Cabeza, L.F., 2012. Review on phase change materials (PCMs) for cold thermal energy storage applications. Appl. Energy 99, 513–533.

OSHA, 2011. Occupational Safety and Health Standards/Hazardous Materials (Standards-29CFR). Occupational Safety & Health Administration.

Otanicar, T., Taylor, R. a., Phelan, P.E., 2012. Prospects for solar cooling - An economic and environmental assessment. Sol. Energy 86, 1287–1299.

Reddy, T.A., Norford, L.K., Kempton, W., 1991. Shaving residential air-conditioner electricity peaks by intelligent use of the building thermal mass. Energy 16, 1001–1010.

Riffat, S.B., Afonso, C.F., Oliveira, A.C., Reay, D.A., 1997. Natural refrigerants for refrigeration and air-conditioning systems. Appl. Therm. Eng.

Rismanchi, B., Saidur, R., BoroumandJazi, G., Ahmed, S., 2012. Energy, exergy and environmental analysis of cold thermal energy storage (CTES) systems. Renew. Sustain. Energy Rev. 16, 5741–5746.

Saito, A., 2002. Recent advances in research on cold thermal energy storage. Int. J. Refrig. 25, 177–189.

Sarbu, I., Sebarchievici, C., 2013. Review of solar refrigeration and cooling systems. Energy Build. 67, 286–297.

Srikhirin, P., Aphornratana, S., Chungpaibulpatana, S., 2000. A review of absorption refrigeration technologies. Renew. Sustain. Energy Rev. 5, 343–372.

Ürge-Vorsatz, D., Cabeza, L.F., Serrano, S., Barreneche, C., Petrichenko, K., 2015. Heating and cooling energy trends and drivers in buildings. Renew. Sustain. Energy Rev. 41, 85–98.

Wang, M.J., Kusumoto, N., 2001. Ice slurry based thermal storage in multifunctional buildings. Heat Mass Transf. 37, 597–604.

LIST OF TABLES

LIST OF FIGURES